Desalination and Water Treatment
www.deswater.com

doi: 10.1080/19443994.2016.1167630

57 (2016) 27226–27236
December

Taylor & Francis
Taylor & Francis Group

KOH-activated carbon developed from biomass waste: adsorption equilibrium, kinetic and thermodynamic studies for Methylene blue uptake

Ramlah Abd Rashid[a,b], Ali H. Jawad[a,b,*], Mohd Azlan Mohd Ishak[a,b], Nur Nasulhah Kasim[a,b]

[a]*Faculty of Applied Sciences, Coal and Biomass Energy Research Group, Universiti Teknologi MARA, 40450 Shah Alam, Selangor, Malaysia, Tel. +60 12 4872038; email: d_chemist@yahoo.com (R.A. Rashid), Tel. +60 49882571; emails: ali288@perlis.uitm.edu.my; ahjm72@gmail.com (A.H. Jawad), Tel. +60 49882027; email: azlanishak@perlis.uitm.edu.my (M.A.M. Ishak), Tel. +60 49882515; email: nurnasulhah@perlis.uitm.edu.my (N.N. Kasim)*

[b]*Faculty of Applied Sciences, Chemistry Department, Universiti Teknologi MARA, Arau Campus, 02600 Arau, Perlis, Malaysia*

Received 20 January 2016; Accepted 15 March 2016

ABSTRACT

In this paper, fallen coconut (*Cocos nucifera*) leaves were used as precursors to prepare activated carbon by thermal carbonization using KOH-activation method. The physical properties of the prepared coconut leaves-activated carbon (KAC) were calculated through the bulk density, ash content, moisture content, and iodine number. The surface characterization of KAC was undertaken using Scanning Electron Microscopy, Fourier Transform Infrared, and point of zero charge (pH_{PZC}) method. Batch mode experiments were performed to assess the influence of the adsorbent dose (0.02–0.25 g), initial pH (3–11), initial dye concentration (30–400 mg/L), contact time (5–300 min), and temperature (303–323 K) on the adsorption of the methylene blue (MB). The kinetic uptake profiles are well described by the pseudo-second-order model, while the Langmuir model describes the adsorption behavior at equilibrium. The adsorption capacity (q_m) of KAC increased with temperature where q_m varied as follows; 147.1 (303 K), 151.5 (313 K), and 151.5 mg/g (323 K). Thermodynamic parameters such as standard enthalpy (ΔH°), standard entropy (ΔS°), and standard free energy (ΔG°) showed that the adsorption of MB onto KAC was spontaneous and endothermic in nature under examined conditions. The results showed the potential use of activated carbon developed from waste coconut leaves for the removal of cationic dye (MB).

Keywords: Activated carbon; Adsorption; Coconut leaves; Methylene blue; Thermal; Potassium hydroxide

1. Introduction

Dye effluents released from dyeing industries, for example textile, paint, pharmaceutical, and cosmetic, have become huge environmental problems. Most of these dyes are highly visible, stable, and resistant to chemical, photochemical as well as biological degradation. Cationic Dyes, which are water-soluble and present as colored cations in solution, and thus frequently referred to as cationic dyes, are applied to paper, polyacrylonitrile, modified nylons, and modified polyesters [1]. Methylene blue (MB) is a cationic dye, which is water soluble and mainly used in industrial activities

*Corresponding author.

such as dyeing of textiles and leather, printing calico, printing cotton, and biological staining methods [2]. The presences of dyes are dangerous since it is non-biodegradable, toxic, accumulates in living organism, and hazardous at high concentration [3]. It has carcinogenic effects and causes various diseases such as allergic dermatitis, skin irritation, dysfunction of kidney, liver, brain, reproductive, and central nervous system [4].

Many treatment methods for the removal of dyes from industrial effluents include adsorption [5,6], bioremediation [7], photocatalysis [8–10], Fenton chemical oxidation [11], electrochemical degradation [12], cation exchange membranes [13], and flocculation–coagulation [14]. Since past several decades, the application of adsorption process has become the focus of intense research and utilization of various conventional [15–17], and non-conventional adsorbents [18–21] are gaining stern consideration. Activated carbon is porous materials that have high surface area and high adsorption capacity and various surface functional groups [22]. It has the ability to remove many pollutants such as dyes, heavy metals, and pesticides. Due to its excellent adsorptive properties, activated carbon is used to purify, detoxify, deodorize, filter, and discolor the concentration of liquid and gas materials. Carbonaceous solid precursor can be used for activated carbon production [23].

Coconut (*Cocos nucifera*) is a palm tree that belongs to the Arecaceae family. The palm tree grows well under warm and humid conditions and is commonly found in tropical and sub-tropical regions. The disposal of the coconut wastes remain a serious problem since it can negatively affect the environment. Several coconut by-products, such as coconut husks [24], shells [25], and dregs residue [26] have been explored as potential precursors for the production of activated carbons. Coconut leaf biomass has limited use and economic value. The waste disposal can be addressed by valorization of these low-cost by-products by conversion into AC. The development of coconut leaf-based AC would address the issues of waste disposal and offer an inexpensive precursor alternative for production.

In our previous work [5], unmodified coconut leaves were successfully used as a potential adsorbent for removal of MB with reasonable adsorption capacity of 112.35 mg/g. The utility of coconut leaves as a precursor led to the current study to produce activated carbon. In particular, the goal of this research was to prepare AC from coconut leaves (KAC) by thermal carbonization using KOH-activation method. Previously, the use of KOH as activating agent has been found to be effective in production of activated carbon with narrow pore size distribution and well-developed porosity [27,28], in addition to the eco-friendly property of KOH [29]. The structural characterization of KAC was performed using scanning electron microscopy (SEM), elemental analysis, and Fourier transform infrared (FTIR), whereas physicochemical parameters were evaluated such as bulk density, ash content, moisture content, iodine number, and point of zero charge (pH_{PZC}). The adsorption properties of KAC at equilibrium and kinetic conditions was studied using Methylene blue (MB) as the model adsorbate at variable adsorbent dosage, initial pH, initial dye concentration, contact time, and temperature for this unique biomaterial.

2. Materials and methods

2.1. Materials

The coconut leaves used for the preparation of activated carbon were collected from Universiti Teknologi MARA (UiTM), Arau Campus, Perlis, Malaysia. The coconut leaves were cut, washed with deionized water to eliminate any contaminants, dried at 100°C for 24 h, grinded and sieved to a particle size of less than 150 μm. Potassium hydroxide (KOH) obtained from HmbG Chemicals was used as the chemical reagent for activation of the coconut leaves. Methylene Blue (MB) dye (chemical formula: $C_{16}H_{18}ClN_3S_3H_2O$, molecular weight: 373.9 g/mol, purity 82%, solubility in water: 40 g/L) purchased from R & M Chemicals was used as the adsorbate. Other chemicals such as hydrochloric acid (HCl), sodium hydroxide (NaOH), iodine, sodium thiosulfate, potassium bromide, and sodium chloride were analytical grade quality.

2.2. Preparation of activated carbon

The coconut leaves were washed thoroughly using tap water to remove any impurities prior to drying in an oven (Memmert, model UFB-400) at 80°C for 48 h. The dried sample was then cut into smaller pieces before grinding into a powdered form (150–212 μm). The coconut activated carbon (KAC) was prepared by mixing KOH with a biomass/KOH impregnation ratio of 1:1 (wt.%) (predetermined as an optimum mixing ratio) with occasional stringing, and then kept in an oven for 24 h at 110°C. The sample was then placed in a stainless steel vertical tubular reactor before carbonizing process in the furnace. The carbonization process was conducted under high purified nitrogen gas (99.99%) with 700°C under the pressure of 1 atm for 1 h. The activated products were then cooled to

room temperature and washed with 3 M of HCl solution and subsequently with hot distilled water until the filtrate turn neutral pH (~pH 7). The KAC was then dried in an oven at 110˚C for 24 h. After that, the KAC was ground and the powder was sieved to obtain a particle size range of 150–212 μm. Finally, the KAC was stored in tightly closed bottles for subsequent use. The physicochemical properties of KAC was calculated through the bulk density, ash content, moisture content, iodine test, and point of zero charge (pH_{PZC}). Bulk density, ash content, moisture content, and iodine number were determined according to procedure described by Ahmed and Dhedan [23], pH_{PZC} is described elsewhere [30].

2.3. Characterization of activated carbon

The scanning electron microscope (SEM) micrographs of the samples were obtained using Quanta (Model Leica Cambridge S360). Fourier-transform infrared (FT-IR) spectrometer (Model Perkin Elmer) was used to verify the presence of surface functional groups before and after adsorption. The proximate analysis of the KAC was performed using a muffle furnace, and the elemental analysis was carried out by using a CHN analyzer (Perkin-Elmer, Series II, 2400).

2.4. Batch adsorption experiments

A predetermined amount of selected adsorbents (0.2 g of KAC) was added to 250 mL Erlenmeyer flasks containing 200 mL of MB solution. The flasks were capped and agitated in an isothermal water bath shaker (Memmert, water bath, model WNB7-45, Germany) at fixed shaking speed of 120 strokes/min and 30˚C until equilibrium was achieved. Batch adsorption experiments were carried out on common variables of interest such as initial pH (3–11), initial dye concentration (30–400 mg/L), and contact time (5–300 min) to determine the optimum conditions for MB adsorption. The pH of MB solution was adjusted by adding either 0.10 M HCl or 0.10 M NaOH to the desired pH value by monitoring with a pH meter (Metrohm, Model 827 pH Lab, Switzerland). After the stirring, the supernatant was collected with a 0.20 μm Nylon syringe filter and the concentrations of MB were monitored at a different time interval using an HACH DR 2800 Direct Reading Spectrophotometer at a wavelength of 661 nm. For the thermodynamic studies, similar procedures were applied at 313 and 323 K, with the other factors keeping constant.

3. Results and discussion

3.1. Physicochemical properties of KAC

The measured physicochemical properties of KAC indicated that KAC has relatively low bulk density (0.16 g/mL), ash content (3.56%), and moisture content (9.37%). This observation indicates that KAC has high carbon content (62.53% form proximate analysis and 73.73% from ultimate analysis), and low volatile matter (24.54%). KAC also gives a good iodine number of 538 mg/g.

3.2. Characterization of KAC

The SEM micrographs of KAC samples before and after MB adsorption are shown in Fig. 1(a) and (b), respectively. The image shows that the surface of KAC before adsorption is highly heterogeneous. Pores with different size and shape are also clearly visible. The pores are produced due to the evaporation of the

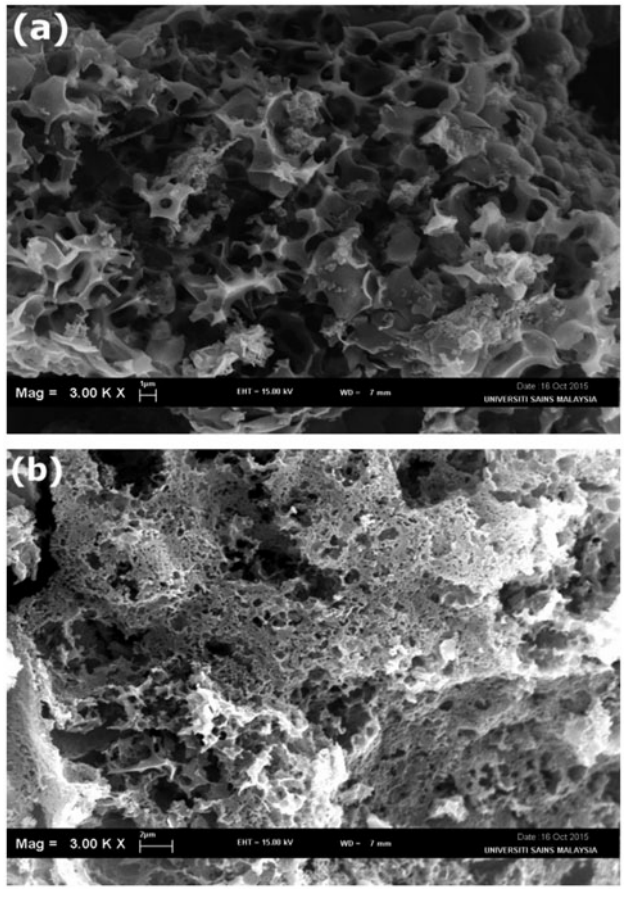

Fig. 1. Typical SEM micrograph of KAC particle (3.0 KX magnifications): (a) before MB adsorption and (b) after MB adsorption.

activating agent from the activated carbon during the activation process [31]. Therefore, large number of MB molecules could easily diffuse and are trapped into the pore structure of KAC. This assumption was supported by Fig. 1(b) where the surface of KAC after MB adsorption became denser and less open pores are seen on the surface of KAC due to loading of MB molecules on the KAC surface.

For the interpretation of functional groups, FT-IR spectral analysis was performed. FT-IR analysis of KAC before MB adsorption in Fig. 2(a) shows bands at 1,550, 1,064, 1,007, and 623 cm^{-1} which are characteristic of stretching vibrations for carboxylate, alkane, secondary cyclic alcohol, and alkene groups, respectively. After MB adsorption as in Fig. 2(b), new peak appeared and many functional groups are either frequency shifted or attenuated. New band appear at 2,884 attributed to the aliphatic C–H stretching such in an aromatic methoxyl group, methyl, and methylene groups of side chains. The peaks at 1,550, 1,007, 814, and 614 shifted to lower bands of 1,546.31, 1,007.50, 814, and 611 cm^{-1}, respectively, while the peak at 879 cm^{-1} shifted to higher bands of 879 cm^{-1}. The possible functional groups of KAC that contribute to interactions with MB cations are the O–H and –COOH groups.

The charge of KAC surface was identified by point of zero charge (pH_{PZC}) analysis. The pH_{PZC} of the KAC was 4.2 (Fig. 3). Below the pH_{PZC} value, surface of KAC is positively charged, favoring the adsorption of anions, and above the pH_{PZC} value the KAC has a negative surface charge, promoting the adsorption of cations.

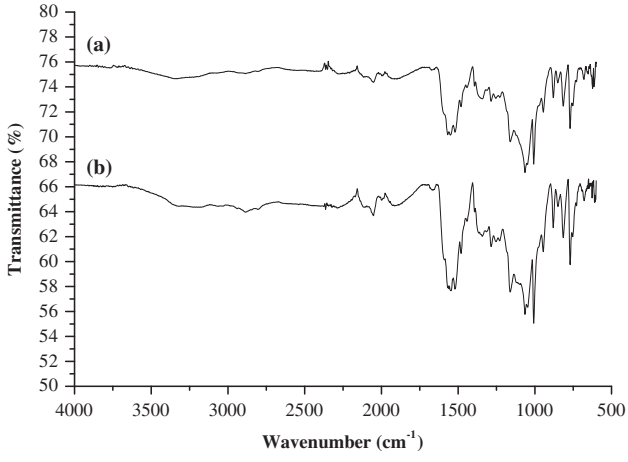

Fig. 2. FT-IR spectra of KAC (a) before MB adsorption and (b) after MB adsorption.

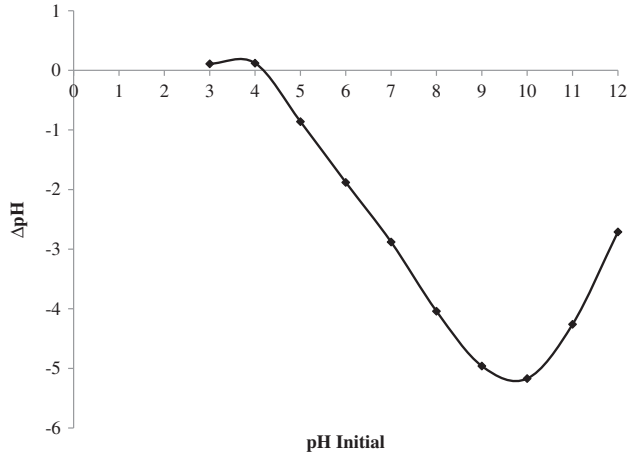

Fig. 3. pH_{PZC} of KAC suspensions.

3.3. Batch adsorption studies

3.3.1. Effect of pH

The pH of the solution influences not only the solution dye chemistry, but also the surface charge of the adsorbent. Fig. 4 illustrates the effect of pH on the adsorption capacity which ranges from pH 3–11. The MB uptake (q_e) onto KAC was not affected by pH within the range due to buffering effect of the adsorbent [32]. Similar observations have been reported for the adsorption of methylene blue by *Parthenium hysterophorus* [33] and sawdust [34]. Therefore, the pH value of unadjusted MB solution (pH 5.6) was used for this study.

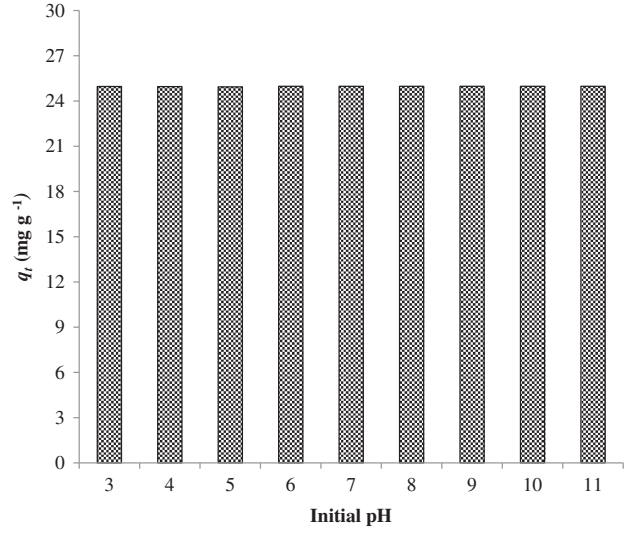

Fig. 4. Effect of pH on the adsorption capacity of MB by KAC. ($[MB]_o$ = 100 mg/L, V = 100 mL, T = 303 K, shaking speed = 120 strokes/min and contact time = 60 min and KAC mass = 0.10 g).

3.3.2. Effect of initial dye concentration and contact time

The effect of adsorption capacity with contact time was investigated with the initial MB concentration that ranged from 30 to 400 mg/L, as shown in Fig. 5. The amount of MB adsorbed on the KAC at equilibrium increased rapidly from 27.6 to 147.5 mg/g with the increase of initial dye concentration from 30 to 400 mg/L. This is attributed to an increase of the collision rate between MB cations and KAC surface at higher initial dye concentration. Hence, more MB cations were transferred to the KAC surface. More time was needed to reach equilibrium at higher dye concentration as there was a tendency for the adsorbate to penetrate deeper within the interior surface of the KAC and occupancy of more active adsorption sites.

3.3.3. Effect of temperature on dye adsorption

Temperature is one of the parameters influenced the adsorption of MB onto KAC. The temperature effect on the adsorption capacity of KAC was tested at 303, 313, and 323 K with the initial concentrations of 30–400 mg/L. Based on the graph plotted in Fig. 6, it is obvious that the adsorption capacity increase with increasing temperature at all MB concentration studied. The adsorption capacity of the KAC increased from 147.1 to 151.5 mg/g as the temperature increased from 303 to 323 K. The observed results in Fig. 6 indicate that the adsorption process of MB onto KAC was favored at higher temperature, in agreement with an endothermic adsorption process.

3.4. Adsorption kinetics

The rate and mechanism of the adsorption process was evaluated using two different kinetic models, namely pseudo-first-order (PFO) model and pseudo-second-order (PSO) model. The PFO model was proposed initially by Lagergren and Svenska [35] and its linearized form is generally expressed by Eq. (1) as follows:

$$\ln(q_e - q_t) = \ln q_e - k_1 t \quad (1)$$

where q_e (mg/g) and q_t (mg/g) are the amount of MB adsorbed by KAC at equilibrium and time t, respectively; while k_1 (1/min) is the PFO model rate constant. The values of k_1 and $q_{e,cal}$ can be determined from the slope and intercept of $\ln(q_e - q_t)$ vs. t, respectively (Fig. 7(a)). The linear form of the PSO model [36] is given by Eq (2):

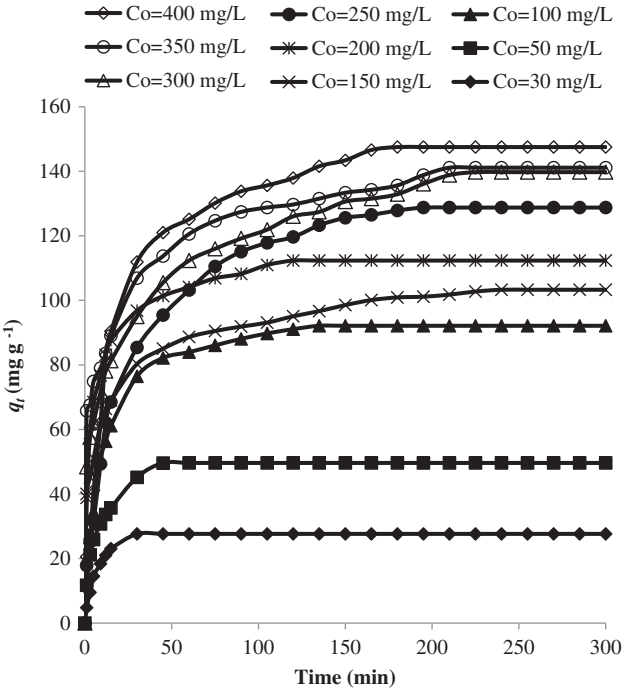

Fig. 5. Effect of initial dye concentration and contact time on the adsorption capacity of MB by KAC. (V = 200 mL, pH 6, T = 303 K, shaking speed = 120 strokes/min, and KAC mass = 0.20 g).

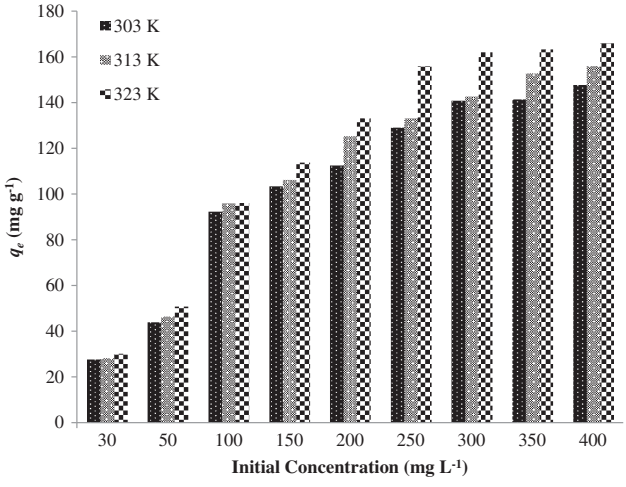

Fig. 6. Effect of temperature on the equilibrium adsorption capacity of KAC at different initial MB concentrations. (V = 200 mL, pH 6, shaking speed = 120 strokes/min and KAC mass = 0.20 g).

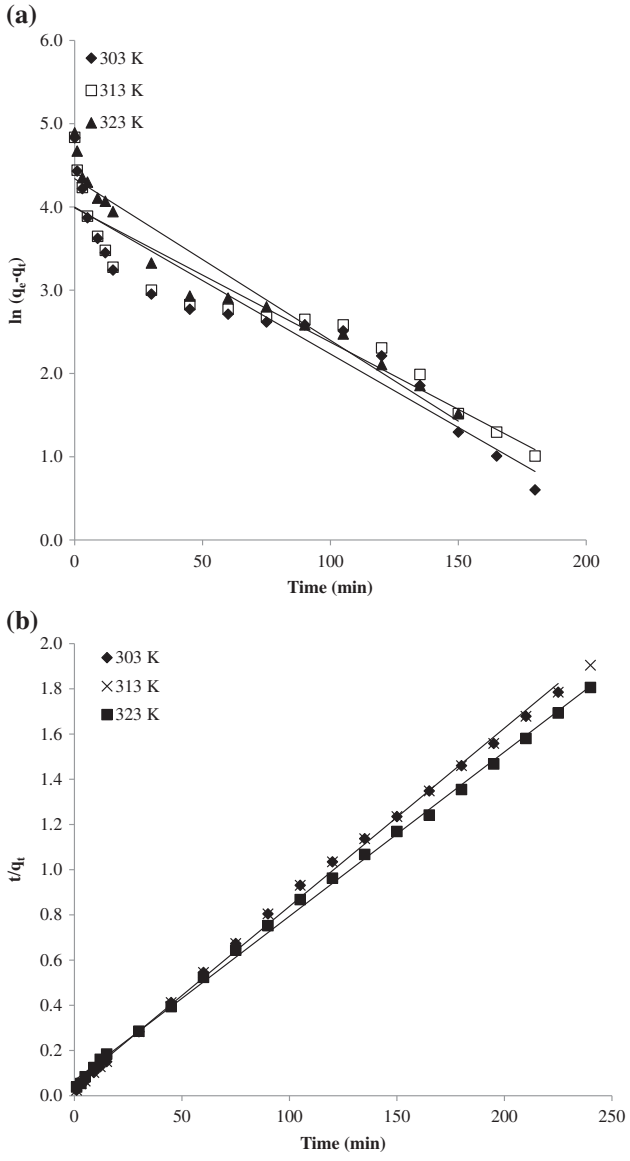

Fig. 7. Kinetic profiles for the adsorption of MB onto KAC at variable temperature: (a) pseudo-first-order and (b) pseudo-second-order.

$$\frac{t}{q_t} = \frac{1}{k_2 q_e^2} + \frac{t}{q_e} \quad (2)$$

where k_2 (g/mg min) is the PSO rate constant. The values of k_2 and $q_{e,cal}$ were calculated from the intercept and slope of t/q_t vs. t, respectively. The plotted graph is shown in Fig. 7(b).

The kinetic parameters of the two models are shown in Table 1 along with its linear regression coefficients, R^2. It can be observed that the R^2 values are greater ($R^2 \geq 0.99$) for the PSO kinetic model. Moreover, its $q_{e,cal}$ values are in agreement with the values of $q_{e,exp}$ Therefore, PSO kinetic model shows a better fit compared to the PFO kinetic model for the adsorption of MB onto KAC surface. The best analysis of kinetic data by the PSO model suggested that the rate-controlling step is chemisorption involving valence forces through the exchange or sharing of electrons between the adsorbate molecules and the surface functional groups of adsorbent [23]. The PSO kinetic model was also implied on adsorption of MB onto activated carbon prepared from palm date seed [37] and apricot stones [38].

3.5. Adsorption isotherms

Adsorption isotherms provide a useful description of the interaction between adsorbates and adsorbents, where the equilibrium distribution of adsorbate molecules occurs between the liquid and solid phases [39]. From the equilibrium data, the linear Langmuir and Freundlich isotherm models were evaluated. Langmuir isotherm [40] describes the monolayer adsorption process for uniform adsorption sites which can be expressed in Eq. (3):

$$\frac{C_e}{q_e} = \frac{1}{q_m K_L} + \frac{1}{q_m} C_e \quad (3)$$

where C_e is the equilibrium concentration (mg/L) and q_e is the amount adsorbed species per specified amount of adsorbent (mg/g), K_L is the Langmuir equilibrium constant, and q_m is the amount of adsorbate required to form an adsorbed monolayer. Hence, a plot of C_e/q_e vs. C_e should be a straight line with a slope ($1/q_m$) and an intercept as ($1/q_m K_L$) as shown in Fig. 8(a).

Table 1
Comparison of the pseudo-first-order (PFO) and pseudo-second-order (PSO) models for the adsorption of MB on KAC at variable temperature

	Temperature (K)		
	303	313	323
$q_{e,exp}$	125.11	122.37	132.88
PFO			
$q_{e,cal}$	48.50	53.90	76.62
k_1 (min^{-1})	0.0167	0.0218	0.0194
R^2	0.921	0.857	0.936
PSO			
$q_{e,cal}$	120.48	128.21	136.99
$k_2 \times 10^{-3}$	0.65	1.19	0.8
R^2	0.992	0.998	0.999

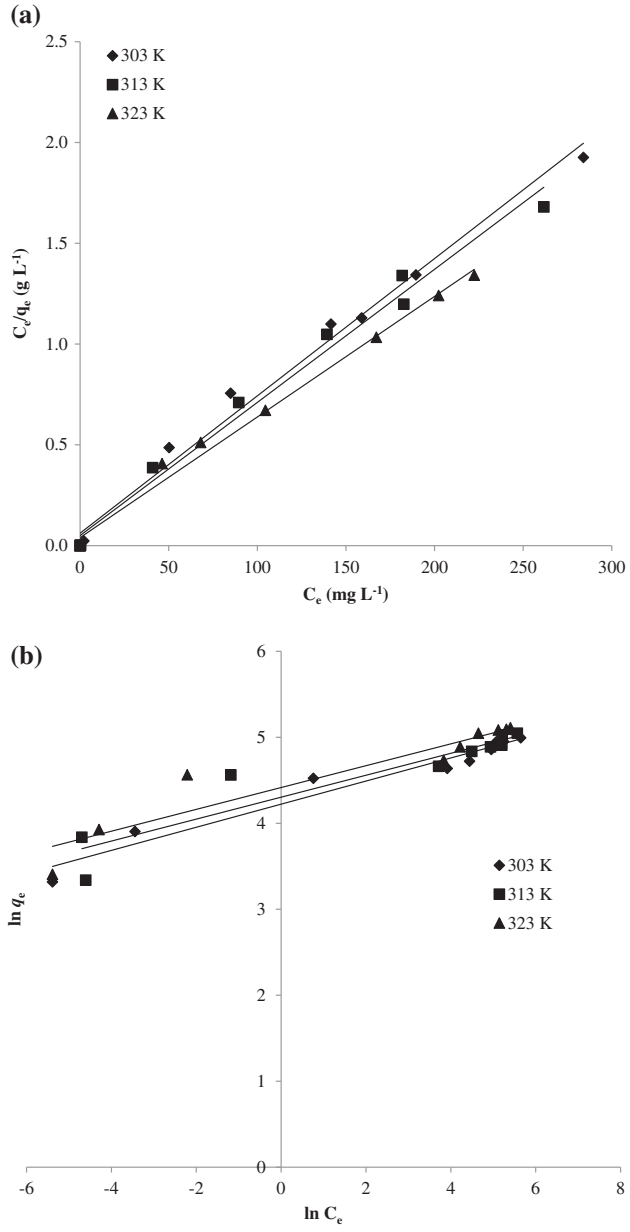

Fig. 8. Langmuir isotherm for the adsorption of MB onto KAC at variable temperature: (a) Langmuir and (b) Freundlich.

Freundlich isotherm [41] describes the multilayer adsorption process on heterogeneous adsorption sites, which can be expressed in Eq. (4):

$$\ln q_e = \ln K_F + \frac{1}{n} \ln C_e \tag{4}$$

where C_e is the equilibrium concentration of the adsorbate (mg/L), q_e is the amount of adsorbate adsorbed per unit mass of adsorbent (mg/g), K_F and n are Freundlich constants where n indicates the relative favorability of the adsorption process. The affinity constant, K_F (mg/g (l/mg)$^{1/n}$, relate to the adsorption capacity of the adsorbent which can also be defined as the adsorption or distribution coefficient, and represents the quantity of dye adsorbed onto activated carbon for a unit equilibrium concentration. The plot of ln q_e vs. ln C_e yields a straight line with slope of $1/n$, whereas; K_F was calculated from the intercept value as illustrate in Fig. 8(b).

The parameters of the these models were calculated and summarized in Table 2 where it is observed that the Langmuir isotherm model provides a better description of the adsorption process according to the R^2 values at all studied temperatures. The results suggest that the adsorption takes place on homogeneous sites that are identical and energetically [42]. KAC shows relatively high adsorption capacities for MB. The calculated q_{max} was found to be 147.1, 151.1, and 151.1 mg/g at temperature of 303, 313, and 323 K, respectively. In addition, the q_{max} of KAC is favorably high in comparison to other activated carbon reported in the literature (*cf.* Table 3). Therefore, KAC has proven here to be an effective adsorbent and should be a possible precursor for the production of activated carbon.

3.6. Adsorption thermodynamics

The adsorption thermodynamic parameters of MB onto KAC were computed from the experimental data conducted at 303, 313, and 323 K. The changes in Gibbs free energy (ΔG°), enthalpy (ΔH°), and entropy (ΔS°) were calculated using the following Eqs. (5)–(7) [22]:

$$K_d = \frac{q_e}{C_e} \tag{5}$$

$$\Delta G^\circ = -RT \ln K_d \tag{6}$$

$$\ln K_d = \frac{\Delta S^\circ}{R} - \frac{\Delta H^\circ}{RT} \tag{7}$$

where K_d is the distribution coefficient, q_e is the concentration of MB adsorbed on KAC at equilibrium (mg/L), C_e is the equilibrium concentration of MB in the liquid phase (mg/L), R is the universal gas constant (8.314 J/mol K), and T is the absolute temperature (K). The values of ΔH° and ΔS° were calculated from the slope and intercept of van't Hoff plots of ln K_d vs. $1/T$, respectively.

The thermodynamic parameters are listed in Table 4. The value for ΔG°, energy for physisorption

Table 2
Isotherm parameters for removal of MB by KAC at variable temperatures

Temperature (K)	Langmuir isotherm		
	q_m (mg/g)	K_L (L/mg)	R^2
303	147.1	0.1099	0.989
313	151.5	0.1325	0.987
323	151.5	0.1667	0.992
	Freundlich isotherm		
	K_F ((mg/g) (L/mg)$^{1/n}$)	$1/n$	R^2
303	68.2	0.134	0.954
313	73.8	0.128	0.874
323	82.8	0.127	0.887

Table 3
Comparison of adsorption capacities for MB adsorption onto different activated carbons prepared by various activation agents

Activated carbon	Activating agent	Adsorbent dosage (g)	pH	Temperature (K)	q_{max} (mg/g)	Refs.
Coconut leaves	KOH	0.10/100 mL	6	303–323	147.1–151.1	This Study
Pistachio nut shell	KOH	0.10/100 mL	10	298	296.57	[43]
Coconut leaves	H_2SO_4	0.15/100 mL	6	303–323	129.9–149.3	[6]
Safflower biochar	$ZnCl_2$	0.40/100 mL	6.5	303	128.2	[44]
Euphorbia rigida	H_2SO_4	0.20/100 mL	6	303	109.98	[45]
Waste apricot	$ZnCl_2$	0.20/100 mL	6	303	102.04	[46]
Cola nut Shells	$ZnCl_2$	0.1/100 mL	6	303	87.12	[47]
Crescentia cujete fruit shell	H_2SO_4	0.2/100 mL	6	303	66.66	[48]
Rosa canina sp. seeds	$ZnCl_2$	0.2/100 mL	6.5	293	47.20	[49]
Sunflower oil cake	H_2SO_4	0.2/100 mL	6	298	10.12	[50]

Table 4
Thermodynamic parameters values for the adsorption of MB onto KAC

Temperature (K)	Thermodynamics parameters				
	k_d	ΔG° (kJ/mol)	ΔH° (kJ/mol)	ΔS° (J/mol K)	E_a (kJ/mol)
303	28.61	−8.95	139.73	490.72	8.43
313	313.03	−13.86			
323	875.67	−18.77			

ranges from −20 to 0 kJ/mol, the physisorption together with chemisorption falls at the range of −20 to −80 kJ/mol and chemisorption is in the range of −80 to −400 kJ/mol [51]. The values of ΔG° of MB adsorption at the temperature of 303, 313, and 323 K were determined as −8.95, −13.86, and −18.76 kJ/mol, respectively. The negative values of ΔG° indicate spontaneous and favorable methylene blue adsorption onto the surface of KAC.

The enthalpy for physisorption is generally below 0 kJ/mol, while for the chemisorption is in the range of −80 to −420 kJ/mol [52]. The calculated ΔH° value was +139.73 kJ/mol, indicating that the adsorption process is endothermic in nature and follows a physisorption mechanism. The positive value of ΔS° (490.72 kJ/mol K) shows that the affinity of KAC to MB and its randomness at the solid/solution interface increases during the adsorption process [53].

3.7. Activation energy of adsorption

The Arrhenius relationship was used to evaluate the activation energy of adsorption representing the minimum energy that reactants must possess for the reaction to proceed:

$$\ln k_2 = \ln A - \frac{E_a}{RT} \quad (8)$$

where k_2 is the rate constant obtained from the PSO model, E_a the Arrhenius activation energy of adsorption, A the Arrhenius pre-exponential factor, R the gas constant, and is equal to 8.314 J/mol K, and T is temperature (K).

The value of E_a range from 5 to 40 kJ/mol indicates a physisorption mechanism. Meanwhile, higher range from 40 to 800 kJ/mol suggests that chemisorption mechanism takes place [54]. According to the experimental E_a (8.43 kJ/mol) obtained, the adsorption of MB on the surface of KAC followed the physisorption mechanism. This physisorption mechanism of methylene blue onto the KAC surface is in agreement with thermodynamic results in Table 4.

4. Conclusion

The results indicated that KAC is an efficient adsorbent for MB adsorption. The optimum adsorption condition can be achieved at 0.2 g of KAC dosage and pH 6.0. The adsorption experiments indicated that the PSO model provided the best kinetic model for the system. On the other hand, the adsorption equilibrium data were better simulated by the Langmuir model with maximum adsorption capacity of 147.1, 151.5, and 151.5 mg/g were obtained at 303, 313, and 323 K, respectively. The thermodynamic parameters indicate that the adsorption process is endothermic and driven by entropy to yield a spontaneous adsorption process.

Acknowledgments

The authors would like to thank the Ministry of Education, Malaysia for funding this research work under the Research Acculturation Grant Scheme (600-RMI/RAGS 5/3(18/2014). The authors also thank the Research Management Institute (RMI) and the Universiti Teknologi MARA for supporting the research work.

References

[1] J. Mittal, A. Mittal, A remarkable adsorbent for dye removal, in: Green Chemistry for Dyes Removal from Wastewater, John Wiley & Sons, Inc., Hoboken, NJ, and Scrivener Publishing LLC, Salem, Massachusetts, 2015, pp. 409–457.

[2] E.N. El Qada, S.J. Allen, G.M. Walker, Adsorption of Methylene Blue onto activated carbon produced from steam activated bituminous coal: A study of equilibrium adsorption isotherm, Chem. Eng. J. 124 (2006) 103–110.

[3] M.J. Ahmed, S.K. Theydan, Physical and chemical characteristics of activated carbon prepared by pyrolysis of chemically treated date stones and its ability to adsorb organics, Powder Technol. 229 (2012) 237–245.

[4] M. Nabil, M. Abbas, A. Zaini, Z. Akmar, Preparation and characterization of activated carbon from pineapple waste biomass for dye removal, Int. Biodeterior. Biodegrad. 102 (2015) 274–280.

[5] A.H. Jawad, R.A. Rashid, R.M.A. Mahmuod, M.A.M. Ishak, N.N. Kasima, K. Ismail, Adsorption of methylene blue onto coconut (*Cocos nucifera*) leaf: Optimization, isotherm and kinetic studies, Desalin. Water Treat. (2015) 1–15, doi: 10.1080/19443994.2015.1026282.

[6] A.H. Jawad, R.A. Rashid, M.A.M. Ishak, L.D. Wilson, Adsorption of methylene blue onto activated carbon developed from biomass waste by H_2SO_4 activation: Kinetic, equilibrium and thermodynamic studies, Desalin. Water Treat. (2016) 1–13, doi: 10.1080/19443994.2016.1144534.

[7] A.R. Khataee, A. Movafeghi, S. Torbati, S.Y. SalehiLisar, M. Zarei, Phytoremediation potential of duckweed (*Lemna minor* L.) in degradation of C.I. Acid Blue 92: Artificial neural network modeling, Ecotoxicol. Environ. Saf. 80 (2012) 291–298.

[8] A.H. Jawad, A.F.M. Alkarkhi, N.S.A. Mubarak, Photocatalytic decolorization of methylene blue by an immobilized TiO_2 film under visible light irradiation: Optimization using response surface methodology (RSM), Desalin. Water Treat. 56 (2015) 161–172.

[9] A.H. Jawad, N.S.A. Mubarak, M.A.M. Ishak, K. Ismail, W.I. Nawawi, Kinetics of photocatalytic decolourization of cationic dye using porous TiO_2 film, J. Taibah Univ. Sci. (2015) 1–11, doi: 10.1016/j.jtusci.2015.03.007.

[10] M.A. Nawi, S. Sabar, A.H. Jawad, Sheilatina, W.S. Wan Ngah, Adsorption of Reactive Red 4 by immobilized chitosan on glass plates: Towards the design of immobilized TiO_2–chitosan synergistic photocatalyst-adsorption bilayer system, Biochem. Eng. J. 49 (2010) 317–325.

[11] Y.S. Woo, M. Rafatullah, A.F.M. Al-Karkhi, T.T. Tow, Removal of Terasil Red R dye by using Fenton oxidation: A statistical analysis, Desalin. Water Treat. 52 (2014) 4583–4591.

[12] L. Fan, Y. Zhou, W. Yang, G. Chen, F. Yang, Electrochemical degradation of aqueous solution of Amaranth azo dye on ACF under potentiostatic model, Dyes Pigm. 76 (2008) 440–446.

[13] J.S. Wu, C.H. Liu, K.H. Chu, S.Y. Suen, Removal of cationic dye methyl violet 2B from water by cation exchange membranes, J. Membr. Sci. 309 (2008) 239–245.

[14] P. Cañizares, F. Martínez, C. Jiménez, J. Lobato, M.A. Rodrigo, Coagulation and electrocoagulation of wastes polluted with dyes, Environ. Sci. Technol. 40 (2006) 6418–6424.

[15] S. Sadaf, H.N. Bhatti, S. Nausheen, S. Noreen, Potential use of low-cost lignocellulosic waste for the

removal of Direct Violet 51 from aqueous solution: Equilibrium and breakthrough studies, Arch. Environ. Contam. Toxicol. 66 (2014) 557–571.
[16] S. Sadaf, H.N. Bhatti, S. Nausheen, M. Amin, Application of a novel lignocellulosic biomaterial for the removal of Direct Yellow 50 dye from aqueous solution: Batch and column study, J. Taiwan Inst. Chem. Eng. 47 (2015) 160–170.
[17] J. Mittal, D. Jhare, H. Vardhan, A. Mittal, Utilization of bottom ash as a low-cost sorbent for the removal and recovery of a toxic halogen containing dye eosin yellow, Desalin. Water Treat. 52 (2014) 4508–4519.
[18] H. Daraei, A. Mittal, J. Mittal, H. Kamali, Optimization of Cr(VI) removal onto biosorbent eggshell membrane: Experimental & theoretical approaches, Desalin. Water Treat. 52 (2014) 1307–1315.
[19] H. Daraei, A. Mittal, M. Noorisepehr, J. Mittal, Separation of chromium from water samples using eggshell powder as a low-cost sorbent: Kinetic and thermodynamic studies, Desalin. Water Treat. 53 (2015) 214–220.
[20] G. Sharma, M. Naushad, D. Pathania, A. Mittal, G.E. El-desoky, Modification of *Hibiscus cannabinus* fiber by graft copolymerization: Application for dye removal, Desalin. Water Treat. 54 (2015) 3114–3121.
[21] A. Mittal, R. Ahmad, I. Hasan, Iron oxide-impregnated dextrin nanocomposite: Synthesis and its application for the biosorption of Cr(VI) ions from aqueous solution, Desalin. Water Treat. (2015) 1–13, doi: 10.1080/19443994.2015.1070764.
[22] J.J. Gao, Y.B. Qin, T. Zhou, D.D. Cao, P. Xu, D. Hochstetter, Y.F. Wang, Adsorption of methylene blue onto activated carbon produced from tea (*Camellia sinensis* L.) seed shells: Kinetics, equilibrium, and thermodynamics studies, J. Zhejiang Univ. Sci. B 14 (2013) 650–658.
[23] M.J. Ahmed, S.K. Dhedan, Equilibrium isotherms and kinetics modeling of methylene blue adsorption on agricultural wastes-based activated carbons, Fluid Phase Equilib. 317 (2012) 9–14.
[24] K.Y. Foo, B.H. Hameed, Coconut husk derived activated carbon via microwave induced activation: Effects of activation agents, preparation parameters and adsorption performance, Chem. Eng. J. 184 (2012) 57–65.
[25] U. Isah, G. Abdulraheem, S. Bala, S. Muhammad, M. Abdullahi, Kinetics, equilibrium and thermodynamics studies of C.I. Reactive Blue 19 dye adsorption on coconut shell based activated carbon, Int. Biodeterior. Biodegrad. 102 (2015) 265–273.
[26] A. Kamari, S.N.M. Yusoff, F. Abdullah, W.P. Putra, Biosorptive removal of Cu(II), Ni(II) and Pb(II) ions from aqueous solutions using coconut dregs residue: Adsorption and characterisation studies, J. Environ. Chem. Eng. 2 (2014) 1912–1919.
[27] L. Khezami, A. Ould-Dris, R. Capart, Activated carbon from thermo-compressed wood and other lignocellulosic precursors, BioResources 2 (2007) 193–209.
[28] T. Kawano, M. Kubota, M.S. Onyango, F. Watanabe, H. Matsuda, Preparation of activated carbon from petroleum coke by KOH chemical activation for adsorption heat pump, Appl. Therm. Eng. 28 (2008) 865–871.
[29] S.E. Abechi, C.E. Gimba, A. Uzairu, Y. Dallatu, Preparation and characterization of activated carbon from palm kernel shell by chemical activation, Res. J. Chem. Sci. 3 (2013) 54–61.
[30] L. Kong, L. Gong, J. Wang, Removal of methylene blue from wastewater using fallen leaves as an adsorbent, Desalin. Water Treat. 53 (2015) 2489–2500.
[31] M. Erdem, T. Tay, S. Karago, Preparation and characterization of activated carbon produced from pomegranate seeds by $ZnCl_2$ activation, Appl. Surf. Sci. 255 (2009) 8890–8896.
[32] K.C. Bedin, A.C. Martins, A.L. Cazetta, O. Pezoti, V.C. Almeida, KOH-activated carbon prepared from sucrose spherical carbon: Adsorption equilibrium, kinetic and thermodynamic studies for Methylene Blue removal, Chem. Eng. J. 286 (2015) 476–484.
[33] H. Lata, V.K. Garg, R.K. Gupta, Removal of a basic dye from aqueous solution by adsorption using *Parthenium hysterophorus*: An agricultural waste, Dyes Pigm. 74 (2007) 653–658.
[34] V.K. Garg, M. Amita, R. Kumar, R. Gupta, Basic dye (methylene blue) removal from simulated wastewater by adsorption using Indian Rosewood sawdust: A timber industry waste, Dyes Pigm. 63 (2004) 243–250.
[35] S. Lagergren, About the theory of so called adsorption of soluble substances, kungl, Svenska Vetenskapsakademien. Handlingar 24 (1898) 1–39.
[36] Y.S. Ho, G. McKay, Sorption of dye from aqueous solution by peat, Chem. Eng. J. 70 (1998) 115–124.
[37] M.A. Islam, I.A.W. Tan, A. Benhouria, M. Asif, B.H. Hameed, Mesoporous and adsorptive properties of palm date seed activated carbon prepared via sequential hydrothermal carbonization and sodium hydroxide activation, Chem. Eng. J. 270 (2015) 187–195.
[38] C. Djilani, R. Zaghdoudi, F. Djazi, B. Bouchekima, A. Lallam, A. Modarressi, M. Rogalski, Adsorption of dyes on activated carbon prepared from apricot stones and commercial activated carbon, J. Taiwan Inst. Chem. Eng. 53 (2015) 112–121.
[39] V.O. Njoku, K.Y. Foo, M. Asif, B.H. Hameed, Preparation of activated carbons from rambutan (*Nephelium lappaceum*) peel by microwave-induced KOH activation for acid yellow 17 dye adsorption, Chem. Eng. J. 250 (2014) 198–204.
[40] I. Langmuir, The adsorption of gases on plane surfaces of glass, mica and platinum, J. Am. Chem. Soc. 40 (1918) 1361–1403.
[41] H. Freundlich, Ueber die adsorption in Loesungen (Adsorption in solution), Z. Phys. Chem. 57 (1906) 385–470.
[42] K.Y. Foo, B.H. Hameed, Preparation, characterization and evaluation of adsorptive properties of orange peel based activated carbon via microwave induced K_2CO_3 activation, Bioresour. Technol. 104 (2012) 679–686.
[43] K.Y. Foo, B.H. Hameed, Preparation and characterization of activated carbon from pistachio nut shells via microwave-induced chemical activation, Biomass Bioenergy 35 (2011) 3257–3261.
[44] D. Angın, E. Altintig, T.E. Köse, Influence of process parameters on the surface and chemical properties of activated carbon obtained from biochar by chemical activation, Bioresour. Technol. 148 (2013) 542–549.
[45] Ö. Gerçel, A. Özcan, A.S. Özcan, H.F. Gerçel, Preparation of activated carbon from a renewable bio-plant of Euphorbia rigida by H_2SO_4 activation and its adsorp-

tion behavior in aqueous solutions, Appl. Surf. Sci. 253 (2007) 4843–4852.
[46] C.A. Basar, Applicability of the various adsorption models of three dyes adsorption onto activated carbon prepared waste apricot, J. Hazard. Mater. 135 (2006) 232–241.
[47] J.N. Nsami, J.K. Mbadcam, The adsorption efficiency of chemically prepared activated carbon from cola nut shells by $ZnCl_2$ on methylene blue, J. Chem. 2013 7 Article ID 469170.
[48] J.A. Joseph, N. Xavier, Equilibrium and kinetic studies of methylene blue onto activated carbon prepared form *Crescentia cujete* fruit shell, Nat. Sci. 11 (2013) 53–58.
[49] A. Gurses, C. Dogar, S. Karaca, M. Acikyildiz, R. Bayrak, Production of granular activated carbon from waste *Rosa canina* sp. seeds and its adsorption characteristics for dye, J. Hazard. Mater. 131 (2006) 254–259.
[50] S. Karagoz, T. Tay, S. Ucar, M. Erdem, Activated carbons from waste biomass by sulfuric acid activation and their use on methylene blue adsorption, Bioresour. Technol. 99 (2008) 6214–6222.
[51] M.J. Jaycock, G.D. Parfitt, Chemistry of Interfaces, Ellis Horwood Ltd., Onichester, 1981.
[52] K.E. Noll, V. Gounaris, W.S. Hou, Adsorption Technology for Air and Water Pollution Control, Lewis Publishers, Chelsea, MI, 1992, pp. 21–22.
[53] I.A.W. Tan, A.L. Ahmad, B.H. Hameed, Adsorption of basic dye using activated carbon prepared from oil palm shell: Batch and fixed bed studies, Desalination 225 (2008) 3–28.
[54] H. Nollet, M. Roels, P. Lutgen, P.V. Meeren, W. Verstraete, Removal of PCBs from wastewater using fly ash, Chemosphere 53 (2003) 655–665.